PHYLLOSILICATES IN BAMBERG CRATER, MARS. C. Gross[1], M. Sowe[1], L. Wendt[1], J. L. Bishop[2] and A. G. Fairén[2] . [1]Freie Universität Berlin, Inst. of Geological Sciences, Malteserstr. 74-100, 12249 Berlin, Germany, christoph.gross@fu-berlin.de. [2]SETI Institute & NASA Ames Research Center, Moffett Field, CA, USA

Introduction: Hydrated silicates have been identified in several impact craters in the northern plains of Mars [1]. Phyllosilicates are of particular interest, because they require relatively long–term liquid water and may represent habitable environments [2]. Most phyllosilicates formed early in Mars' history during the Noachian period [3]. Phyllosilicate outcrops in the northern plains are exclusively found in and around impact craters [1]. This leads to the conclusion that they must be excavation products of preexisting, buried deposits, exposed by impacting and erosion [1-5]. However, the Hesperian–aged Toro crater bears evidence for impact–induced hydrothermal mineralizations [2,5,6]. Aqueous solutions and volatile components interacted there with the hot and brecciated rocks, leading to alteration and hydrothermal overprinting of the area and to the deposition of secondary minerals. Extensive modeling was carried out by [7] to determine the extent of hydrothermal circulation and discharge of waters after an impact, even under current Martian conditions for crater sizes between 45 km and 90 km in diameter. Other possibilities for phyllosilicate formation include weathering, even under arid conditions over a long period of time [8] or sedimentary processes [9]. Here, we investigate the Bamberg impact crater, located at 39.71°N 356.9°E, north of Arabia Terra.

Geologic Setting and Study Area: Bamberg is a ~55 km-diameter impact crater located in the northern hemisphere, roughly 60 km north of the highlands/lowlands boundary, in the southern Acidalia Planitia region, close to the transition to the Arabia Terra region [10]. The crater shows relatively well preserved terraced walls and a distinct ejecta blanket suggesting the possible presence of water-ice and volatile-rich target materials. The most prominent feature of the crater is the central uplift, displaying an asymmetric central pit, again suggesting the precence of volatiles in the subsurface [11,12]. The central peak has a diameter of ~15 km and its central pit has an extension of ~7 km in the east-west and ~5 km in the north-south directions. Several pristine looking gullies can be observed on the southern and western walls of the central pit, whereas the remaining part of the pit displays a blocky texture. Some sporadic outcrops of megabreccia can be recognized on the northern wall of the pit. At the bottom of the pit, convoluted dark toned and ridge like structures are observed, covered by light toned dune material.

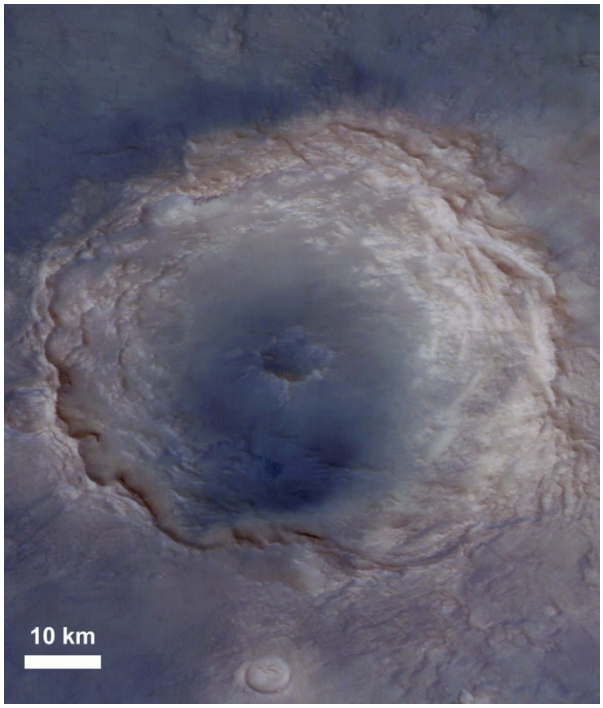

Figure 1: Bamberg Crater shown by HRSC, nadir with IR-G-B channels (h7504_0000).

Data Sets and Methods: Visual interpretations were carried out using HRSC, CTX, HiRISE and THEMIS data. We used CRISM image FRT0000942F with a spatial resolution of 18 m/px [13]. We focused our analyses on spectra from 1-2.6 µm where hydrated minerals such as phyllosilicates exhibit representative absorptions. The band near 1.9 µm is indicative of H_2O in minerals, whereas OH combination bands and overtones in clay minerals have diagnostic absorptions at 2.1-2.5 µm [14]. CRISM Analysis Toolkit (CAT) and its associated tools were used in ENVI to minimize instrumental and atmospheric effects and convert the data to I/F [15,16]. Spectra were collected for 5x5 pixel spots and ratioed in column to emphasize the mineral features (Fig. 2). Laboratory spectra of the CAT RELAB have been used for comparison with the Martian spectra.

Results: In general, the spectral summary parameters show a strong olivine signature, high calcium pyroxene and D2300 abundance (pointing to Fe/Mg-OH minerals) along the rim of the central peak (light-toned) and on its slopes (smooth dark toned units).

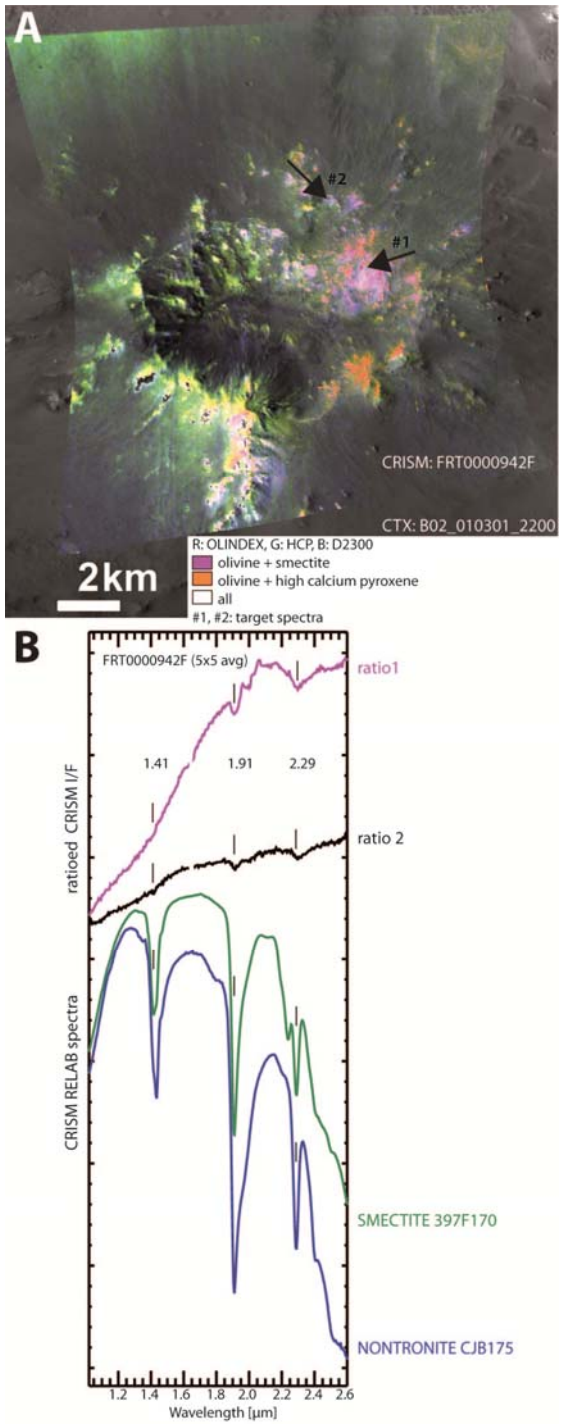

Figure 2: CRISM I/F spectra of hydrated mineral draped on CTX (A) and lab spectra of Fe-rich smectites that best match the hydrated outcrops (B).

Olivine-rich and hydrated units often coincide (magenta in Fig. 2A). However, olivine is more abundant and has a strong signature in the light-toned units. Ratioed spectra of the hydrated outcrops have absorptions at ~1.41, 1.91 and 2.29 µm, best matching the Fe-smectite nontronite. Chlorite was previously identified in Bamberg crater [1] but is inconsistent with our spectra due to the presence of a 1.9 µm H_2O band. However, the Bamberg spectra exhibit only weak bands due to OH and H_2O, precluding unique phyllosilicate determinations. Possibly a mixed layered smectite/chlorite (S/C) [17] could be present as well with a high smectite component. Nontronite is an iron(III)-rich member of the smectite group and is most commonly formed from weathering of basalts, kimberlites and other ultramafic rocks [8,9,14]. Nontronite can be found in joints and fractures, as coating and also as pseudomorphosis of hornblende and pyroxene. Nontronite is also found as impregnation in porous country rock of olivine basalts. Furthermore, nontronite can be found in hydrothermal environments such as deep sea ventstructures [18], for example oceanic ridges. Authigenic formation also takes place in marine sediments.

Conclusions: The observed mineral assemblages in Bamberg do not point to a conclusive mode of formation for the phyllosilicates. The presence of diverse megabreccia in the areas of interest could indicate an ancient derivation as described by [19]. Nevertheless, Bamberg remains an interesting target for further studies.

Acknowledgements: This work has been partially supported by the DFG Grant NE 212/11–1, by the Helmholtz Association through the research alliance “Planetary Evolution and Life” and by the German Aerospace Agency (DLR) in context with the Mars Express project.

References: [1] Carter J. et al. (2010) *Science 328*, 1682-1686. [2] Fairén A. G. et al. (2010) *Proc. Natl. Acad. Sci. 107 (27)*, 12095–12100. [3] Bibring J.–P. et al. (2006) *Science, 312*, 400-404. [4] Murchie S. L. et al. (2009) *J. Geophys. Res., 114*, doi:10.1029/2009 JE003342. [5] Fairén A. G. et al. (2011) Nat. Geos., 4, 667-670. [6] Marzo G. A. et al. (2010) *Icarus, 208*, 667–683. [7] Barnhart C. J. et al. (2010) *Icarus 208*, 101-117.[8] Velde B. (1995) *Origin and Mineralogy of Clays*. Springer-Verlag, Berlin. [9] Chamley H. (1989) *Clay Sedimentology*. Springer-Verlag, New York. [10] Webb V. E. (2004) *J. Geophys. Res., 109*, doi:10.1029 /2003JE002205. [11] Carr M. H. (1977) *Proc. Symp. Planet. Crat. Mechanics*, 593-602. [12] Barlow N. G. and Perez, C. B. (2003) *J. Geophys. Res. 108*, 5085. [13] Murchie S. L. et al. (2009) *J. Geophys. Res. 114*, doi:10.1029/2009JE 003344. [14] Bishop, J. L. et al. (2008) *Clay Minerals 43*, 35-54. [15] Murchie S. L. et al. (2009) *J. Geophys. Res. 114*, doi:10.1029/2009JE 003342. [16] McGuire P. C. et al. (2009) *Planet. Space Sci. 57*, 809–815. [17] Milliken, R. E. et al. (2010) 2010LPI....41.2030M. [18] Halbach, P. E. et al. (2003) *Energy and Mass Transfer in Marine Hydrothermal Systems*, Dahlem University Press, 85-122. [19] Ehlmann, B. L. et al. (2011) *Nature 479*, 53-60.